Med Biol Eng Comput
DOI 10.1007/s11517-008-0309-z

ORIGINAL ARTICLE

On arousal from sleep: time-frequency analysis

M. O. Mendez · A. M. Bianchi · N. Montano · V. Patruno · E. Gil · C. Mantaras · S. Aiolfi · S. Cerutti

Received: 9 July 2006 / Accepted: 21 January 2008

Abstract Time-frequency analysis of the heart rate variability during arousal from sleep, with and without EMG activation, coming from five obese healthy subjects was performed. Additionally, a comparative analysis of three time-frequency distributions, smooth pseudo Wigner–Ville (SPWVD), Choi–Williams (CWD) and Born–Jordan distribution (BJD) is presented in this study. SPWVD showed higher capacity for eliminating the cross terms independently of the signal. After applying Hilbert transformation to real signals BJD and CWD lost some important mathematic properties as marginals, on the contrary PSWVD remains unchanged. BJD showed results comparable with CWD. During arousal episodes, analogous energy distribution and spectral indexes were obtained by the three time-frequency representations. Arousals with chin activity presented stronger changes in RR intervals and LF (related to sympathetic activity) component, being statistically different with respect to arousal without chin activity, only around the period of maximum change in β activity on the EEG. These results suggest a more evident stress for the heart when an arousal is related to external muscular activity.

Keywords Heart rate variability · Arousal from sleep · Time-frequency distributions · Sleep fragmentation · Autonomic nervous system

M. O. Mendez (✉) · A. M. Bianchi · S. Cerutti
Department of Biomedical Engineering, Politecnico di Milano, P.zza Leonardo da Vinci 32, 20133 Milan, Italy
e-mail: martin.mendez@biomed.polimi.it

N. Montano
Department of Clinic Science, University of Milan, Ospedale L. Sacco, Milan, Italy

V. Patruno · S. Aiolfi
Hospital Unit of Respiratory Rehabilitation, Ospedale S. Marta, Ospedale Maggiore di Crema (CR), Rivolta D'adda, Italy

E. Gil
Communication Technology Group, University of Zaragoza, Zaragoza, Spain

C. Mantaras
Department of Biomedical Engineering, Fac. Ingeniería, Universidad Nacional de Entre Ríos, Parana, Argentina

1 Introduction

In the last few years, arousal from sleep has been one of the most studied sleep phenomena related to sleep fragmentation. Sleep fragmentation is associated with several symptoms, ranging from somnolence, excessive daytime sleepiness, impaired learning, reduced memory capabilities [31] and up to much more severe consequences such as cardiovascular diseases. When sleep fragmentation is associated with sleep-disordered breathing [47, 48], such as obstructive sleep apnea (OSA), there is a high-likelihood to develop arterial hypertension and other cardiovascular diseases [9, 17, 46, 48].

Arousals are normally scored from either the central or the occipital leads of the electroencephalogram (EEG) during standard polysomnographic studies. An arousal consists in "an abrupt shift in EEG frequency, which may include θ, α and/or frequencies greater than 16 Hz but not spindles" [1]. Different studies have been carried out in order to understand the physiologic effects of arousals. Some examples of the experimental protocols used during arousal studies include: inducted arousals at different intensities and periodicities during sleep as well as arousals after sleep deprivation [8, 11, 18, 19, 33, 40]. A number of

studies reported that arousal generates a typical waveform in the heart rate (HR), which consists in an abrupt increment followed few seconds later by a decrement in HR [9, 33, 40].

Spectral analysis of the heart rate variability (HRV) signal represents a powerful noninvasive tool for evaluating the action of the autonomic nervous system (ANS). It is widely known that power spectral density (PSD) of the HRV exhibits oscillations, which are related to the parasympathetic and sympathetic activities. Wide band of spectral components of the HRV goes from 0.003 to 0.5 Hz, where the range between 0.003 and 0.04 Hz (very low-frequency component, VLF) takes account of long-term regulation mechanisms; the range between 0.04 and 0.15 Hz (low-frequency component, LF) represents both sympathetic and parasympathetic modulation [24, 32], but an increase in its power is generally associated to a sympathetic activation. However, even nowadays, there is a controversy about the contribution of each autonomic branch to this frequency band. The 0.15–0.5 Hz range (high-frequency component, HF) corresponds to parasympathetic modulation and it is synchronous with respiratory rate [45]. Finally the low to high frequency ratio is a concise index to evaluate the sympatho-vagal balance [29] controlling HR.

So far, most of the studies have investigated the effects that arousals produce on the cardiovascular system by using time domain or Fourier transform (FT) techniques. Only few works applied more sophisticated techniques such as time-varying analysis, to evaluate the dynamic changes of the cardiovascular control during arousals [6]. To this regard, we focused our attention on a special and well-known set of tools called Cohen's class time-frequency distributions (TFDs) [16].

The purposes of this study are: (1) to evaluate the ability of different time-frequency distributions including smooth pseudo Wigner–Ville distribution (SPWVD), Choi–Williams distribution (CWD) and Born–Jordan distribution (BJD), in assessing the temporal dynamics of the autonomic control during spontaneous arousals and (2) to assess cardiac autonomic control during arousals associated or not to muscular activity using the most adequate approach according to (1).

2 Methodology

During constant physiological conditions, the HRV signal is stationary, thus application of Fourier transform or autoregressive batch analysis gives adequate spectral description of the signal. However, when it is necessary to analyze rapid changes in the signal (transients), such as the HRV variations during Valsalva maneuver, apneas and arousals, these approaches are not the most suitable. In order to overcome this inconvenience, other techniques such as, short time Fourier transform [22], discrete wavelet analysis [28], time-varying analysis [4] and quadratic time-frequency distributions [16, 22], have been introduced. Previous studies obtained interesting inferences on neural control of circulation, by applying these mathematical methods to the HRV analysis in different cardiovascular diseases and sleep disorders [3, 5, 34, 36, 43].

2.1 Time-frequency distributions

Cohen's class time-frequency distributions of a signal $x(t)$ have the special characteristic of being time and frequency shift invariant and are generally defined as:

$$C_x(t,f) = \iint \varphi(t-t',\tau)x*\left(t'-\frac{\tau}{2}\right)x\left(t'+\frac{\tau}{2}\right)\mathrm{e}^{-j2\pi f\tau}\mathrm{d}t'\mathrm{d}\tau \tag{1}$$

where $\varphi(t-t',\tau)$ is a function labeled kernel. By choosing different kernels, different features of the distributions are obtained. The function of the kernel is to reduce spurious components generated by the quadratic nature of the distribution. Those are called cross-terms and disturb the energy signal interpretation in the time-frequency plane. For the HRV analysis, the most used distributions in literature are: smooth pseudo Wigner–Ville distribution and Choi–Williams distribution. Another distribution frequently used in literature is the Born–Jordan distribution. All these distributions come from the Cohen's class and are defined as in the following according to the kernel $\varphi(t,\tau)$.

2.1.1 Smooth pseudo Wigner–Ville distribution

$$\varphi(t,\tau) = \gamma(t)\eta\left(\frac{\tau}{2}\right)\eta^*\left(-\frac{\tau}{2}\right) \tag{2}$$

This distribution was introduced by Martin W. and Flandrin P. in 1985 [30] and is characterized by independent smoothing functions in time and frequency, originated by $\gamma(t)$ and $\eta\left(\frac{\tau}{2}\right)\eta^*\left(-\frac{\tau}{2}\right)$ windows, respectively.

2.1.2 Choi–Williams distribution

$$\varphi(t,\tau) = \sqrt{\frac{\sigma}{4\pi}}\frac{1}{\tau}\exp\left[-\frac{\sigma}{4}\left(\frac{t}{\tau}\right)^2\right] \tag{3}$$

It was introduced by Choi and Williams in 1989 [14]. The scaling factor σ determines the cross-term suppression, time and frequency resolution and the auto-terms concentration. High values of σ give good auto-terms definition

and low cross-terms suppression, while low values of σ reduce cross-terms and spread out the auto-terms.

2.1.3 Born–Jordan distribution

$$\varphi(t,\tau) = \begin{cases} \frac{1}{|\tau|}, & |t/\tau| < 1/2 \\ 0, & |t/\tau| > 1/2 \end{cases} \quad (4)$$

This distribution has attractive properties since it associates mixed products of time and frequency domains [15]. The distribution had been used as basis for creating other distributions or for evaluating new distributions [25, 27, 44].

2.2 Basic properties of the time-frequency distributions

Detailed and extensive description of the distribution properties, connected to a specific kernel is reported in literature [16, 22]. In the present section, we only recall a brief summary of the most important properties that a kernel should satisfy in order to be useful for the time-frequency analysis of biomedical signals:

Property 1—the TFD should be real valued, and as a consequence, the kernel must satisfy the relation:

$$\varphi(t,\tau) = \varphi^*(t,-\tau)$$

Property 2—the TFD should attain the marginals. In other words, if we integrate the TFD with respect to the time axis, we should obtain the power spectrum of the signal in the frequency domain. Furthermore, if the integration is carried out with respect to the frequency axis, the result should be the instantaneous power as a function of time.

$$\int C_x(t,f)\mathrm{d}t = |X(f)|^2$$

$$\int C_x(t,f)\mathrm{d}f = |x(t)|^2$$

Where $X(f)$ is the Fourier transform of the signal $x(t)$. This is obtained only if the kernel satisfies the following relations:

$$\varphi(t,0) = \delta(t) \quad \text{and} \quad \int \varphi(t,\tau) = 1$$

where $\delta(t)$ is the Dirac's Δ function.

Property 3—the TFD should satisfy the finite support, this implies that the kernel should be zero in the time and frequency regions where the signal does not exist.

$$\begin{array}{llllll} C_x(t,f) = 0 & & \text{when} & & & \\ x(n) = 0 & \text{for} & t < t_1 & \text{and} & t > t_2 & \\ X(f) = 0 & \text{for} & f < f_1 & \text{and} & f > f_2 & \end{array}$$

This will be obtained if the kernel attains:

$$\varphi(t,\tau) = 0 \quad \text{for} \quad |t| > |\tau|$$

2.3 Synthetic signal

The analysis of these mathematical approaches is illustrated by using a synthetic bi-component signal $s(n)$, which is formed by summing up a sinusoid and a Gaussian function. The synthetic signal structure is defined as follows:

$$s(n) = \sin(2\ \pi\ fn) + \frac{1}{\sigma\sqrt{2\ \pi}} \mathrm{e}^{\left(\frac{(n-\mu)^2}{2\sigma^2}\right)}$$

where n is time, $f = 0.25$ Hz and $\sigma = 3.5$. Sinusoid function is defined for $1 \leq n \leq 512$ and Gaussian function for $92 \leq n \leq 319$, zero otherwise. Gaussian function was modulated with a frequency equal to 0.05 Hz.

The frequency value of the sinusoid was assigned similar to the respiratory frequency, while the duration (20 s) of the Gaussian function was chosen in order to reproduce approximately the duration of an arousal. The analysis is limited to this simple synthetic signal that allows to assess the capabilities of the different TFDs in analyzing the ANS behavior during physiological conditions.

Sampling frequency of the synthetic signal was 4 Hz with 512 samples as duration. TFD parameters were chosen on the basis of recommendations and experimental results reported in previous studies. For SPWVD [28, 34, 35]: smoothing time window was a Hamming of 21 samples and smoothing frequency window was a Hamming of 129 samples. For CWD [39]: fixed value of $\sigma = 1$.

Three frequency bands: A (0.35–0.45 Hz), B (0.2–0.3 Hz) and C (0.05–0.1 Hz) were selected in order to have an indication of the cross-term and auto-term amplitudes. Each band and the total frequency range (0–0.5 Hz) were integrated across the frequency axis for comparing with the theoretical instantaneous power of the signal. In a second step, we applied the Hilbert transform to the real signal in order to evaluate how much the cross-terms are reduced and the mathematical properties of the TFDs are maintained.

2.4 Arousal from sleep data

2.4.1 General procedures

Five overnight polysomnographic recordings were obtained from healthy subjects screened for obstructive sleep apnea. Table 1 shows the clinical data for all subjects. Data were obtained by a polymnosograph heritage

Table 1 Clinical data of the subjects included in the study

Subject	Sex	Age	BMI	Weight (kg)	Height (m)	Total sleep time (h)	Sleep efficiency (%TIB)
1	F	53	37	100	1.64	6.14	93
2	M	50	35	88	1.58	6.4	95
3	M	47	35	98	1.67	6.25	92
4	M	50	36	95	1.63	6.49	96
5	M	49	38	103	1.64	6.32	92

REM (%TST)	S1 (%TST)	S2 (%TST)	SWS (%TST)	Arousal index (%TST)	Total arousals	Arousals included in the study	
						With EMG	Without EMG
22.5	14.1	44.5	18.9	5.2	32	3	2
20	5.3	37.7	37	6	38	3	3
20	8.6	45	26.4	2.7	17	2	1
31	9.6	35.8	23.6	11.6	75	5	5
20.1	20.1	36.3	23.6	3.6	23	4	3

S1, *S2* mean sleep stages 1 and 2, respectively; *SWS* slow wave sleep; *TST* total sleep time

digital PSG grass telefactor with 100 Hz as sampling frequency. Recorded variables were oxygen saturation, body position, two encephalographic derivations (C4/A1 and O1/A2), chin electromyogram (EMG), left and right electrooculogram (EOG), leg movement, airflow, thoracic and abdominal respiratory movements and electrocardiogram (ECG).

2.4.2 Protocol

Sleep stages were evaluated according to the standard criteria [37], only C4/A1 EEG channel, ECG and chin eletromyogram were used in the present analysis. Arousals were identified from EEG channel during stage 2, in agreement with the definition given in [1]. The arousals were semi-automatically detected by an algorithm described below and then checked by an expert. We restrained arousal definition to a closed and limited group of arousals, which are characterized by duration between 3 and 6 s. Further, the included arousals were not preceded by k-complexes. The arousals were detected as follows:

- EEG channel was filtered by a low-pass filter with cut frequency of 30 Hz.
- Four filters, with 0–4, 4–8, 8–13 and 16–30 Hz as pass bands, were used to separate δ, θ, α and β cerebral activity components, respectively.
- β and θ components were squared and smoothed with a moving average filter (100 points).
- From smoothed β rhythm, only events higher than a threshold (200% higher than the previous 10 s) value and with a time duration between 3 and 6 s were taken as arousal.
- Arousals were classified in to two groups: (1) EEG shift frequency and (2) EEG shift frequency and muscular activity.
- A new arousal was identified at least 40 s after the end of the previous one.
- Arousals close at least 120 s to a sleep stage change were not considered.
- Arousal detection was based on the rectified β rhythm, after this process, expert clinical personal revised the identified arousals.

Fourteen arousals without muscular activity and 17 with muscular activity were selected which were not associated to sleep events. Then, the RR interval was detected from the ECG channel through a derivative algorithm. Due to the low sampling frequency, a better detection of the *R* peaks was obtained by parabolic interpolation [4]. When extra-systoles happened, the corresponding portion of the signal was discarded. The minimum RR value during the arousal event (corresponding to the β-increment) was taken as reference point. A time window of 90 s (30 s before and 60 s after the reference point, RR minimum value) was considered for the analysis.

2.4.3 Spectral analysis

Resulting RR sequences were re-sampled at 2 Hz by cubic spline interpolation and detrended by subtracting the mean value. Then, Hilbert transform was applied to the RR sequences to obtain an analytic signal. After that, SPWVD was used to obtain the RR power at different frequencies and times. We decided to use this distribution on the basis of a comparative analysis performed on the synthetic

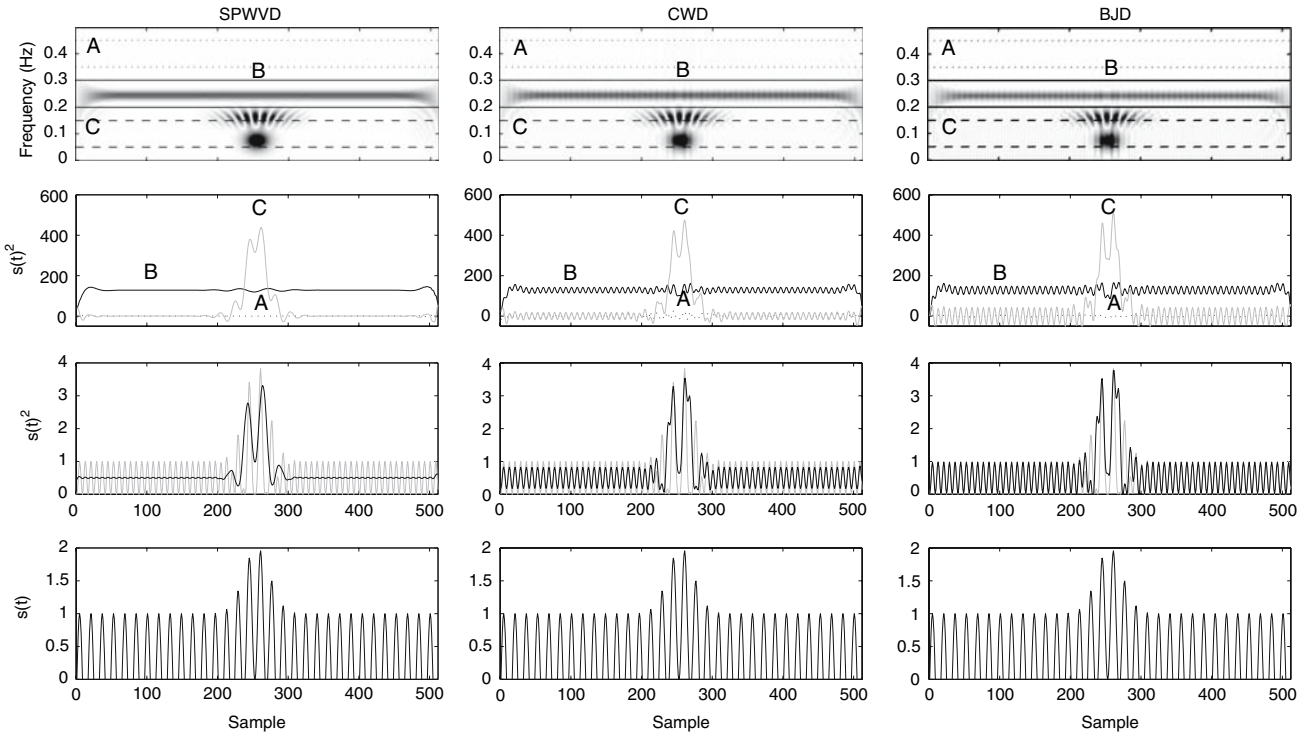

Fig. 1 Time-frequency analysis of the synthetic signal. The first row shows the time evolution of the PSDs of the signal obtained through three time-frequency representations: smooth pseudo Wigner–Ville distribution (SPWVD), Choi–Williams distribution (CWD) and Born–Jordan distribution (BJD). The second row depicts the instantaneous power for A (*dashed line*), B (*black line*) and C (*gray line*) frequency bands. The third row presents the instantaneous power for the whole frequency axis, *gray line* represents the theoretical instantaneous power while *black line* is the one obtained after integrating the PSD with respect to the frequency axis

signals, which is also presented in the result section. Total power, VLF, LF, HF power and LF/HF have been calculated for each sample in the RR sequence. The time-frequency representations and the spectral indexes were obtained using the absolute values of the distributions.

2.4.4 Data analysis

Time series segments of 90 s during arousals were analyzed. RR intervals and the time series of the spectral indexes corresponding to each arousal were normalized as percentage of relative changes in respect to a baseline, where the baseline was obtained averaging the first 20 s of each sequence (baseline before the arousal). All the indexes are expressed as mean ± standard error (SE). In addition, all the indexes were divided in four phases defined as: "0" average of five beats occurring 10 s before the RR minimum, "1" average of three beats centered around the RR minimum, "2" average of four beats occurring 5 s after the RR minimum and "3" average of ten beats occurring 15 s after RR minimum. These intervals were selected as key points that could characterize the arousal episode in the RR interval.

One-way ANOVA for repeated measures was performed to compare the indexes in time with respect to the reference value. Bonferroni's post-hoc analyses were performed to estimate significant differences ($p < 0.05$). Two groups *t*-test was used to compare arousals with muscular or without muscular activity.

3 Results

3.1 Synthetic signal analysis

The energy content at different times and frequencies of the synthetic signal is shown in Fig. 1. All the TFDs are able to separate the signal components. However, BJD shows a higher number of cross-terms coming from the perpendicular relation between the auto-terms located in the negative and positive frequencies. It is worth noting that the cross-terms maintain the marginal properties of the TFD. The three TFDs tracked accurately the frequency changes along the time.

Figure 2 shows the results of the TFDs for the analytic version of the synthetic signal. One can observe that the SPWVD does not show perceptible visual changes in the energy distribution between analytic and real signal version. For analytic signal, the CWD and BJD present very noticeable changes in their graphical representation of the

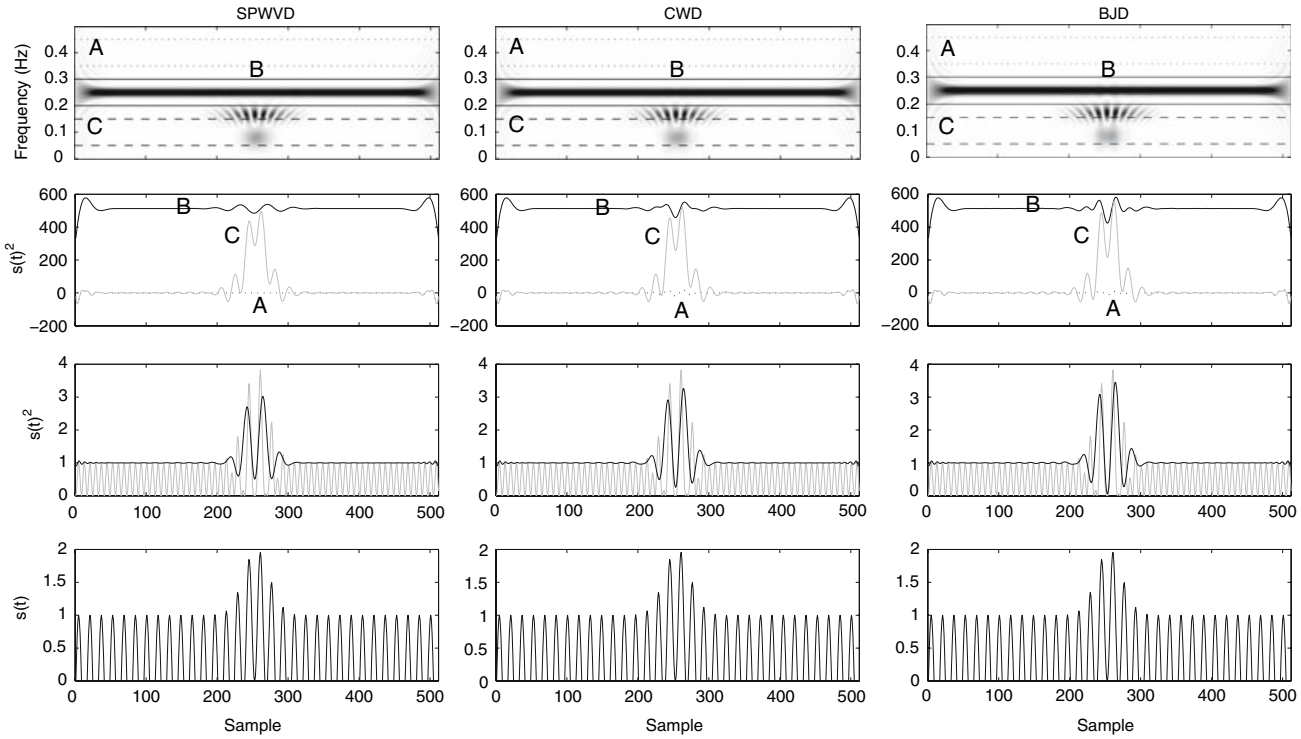

Fig. 2 Time-frequency analysis of a synthetic signal, after the Hilbert transformation. The first row shows the time evolution of the PSD of the signal obtained by three time-frequency representations, Smooth pseudo Wigner–Ville distribution (SPWVD), Choi–Williams distribution (CWD) and Born–Jordan distribution (BJD). The second row depicts the instantaneous power for A (*dashed line*), B (*black line*) and C (*gray line*) frequency bands. The third row present the instantaneous power for the whole frequency axis, *gray line* represents the theoretical instantaneous power while *black* line is the one obtained after integrating the PSD with respect to the frequency axis

energy content. In addition, the cross-terms are almost completely removed and the marginal properties were not preserved since the TFDs are not able to follow time by time the instantaneous power of the signal (see Fig. 2, row 3). The three TFDs seem to have the same performance when an analytic signal is analyzed. If we compare the row 2 of Figs. 1 and 2, the powers in band B show a clear increment, meaning that the auto-terms are more concentrated in the time-frequency plane and the cross-terms reduced.

3.2 Arousal analysis

Figure 3 depicts the energy distribution of the RR interval sequence during an arousal using SPWVD, CWD and BJD. One can observe, in the second column (real signal), that all TFDs disjoin perfectly the spectral components of the RR interval but CWD and BJD present higher cross-terms spreading across the frequency axis. The results of the TFDs, for analytic version are shown in column one. It is possible to note small residuals of cross-terms on CWD and BJD.

Finally, on the basis of these previous results, we decided to use SPWVD for the analysis of the RR sequences.

Figure 4 displays the spectral indexes of the HRV for 17 arousals with (black symbols) and 14 arousals without (gray symbols) muscular activity. The values are represented as the percentage of change with respect to a baseline. The figure shows around 20 s before and after the RR minimum value in order to observe the arousal effects on the HRV indexes. RR interval decreases and reaches the minimum value 7 s after the initial increment in the cerebral β activity. Then the recovery phase starts going up to the baseline and returning to the baseline 15 s later during arousals with muscular activity. RR interval decreases showing significant lower values with respect to baseline in the time interval between 14 and 22 s, while during arousals without muscular activity, there are significant differences with respect to the baseline only within the time interval between 18 and 19 s. The second subplot shows the time evolution of the rectified β activity: Both groups of arousals present the same characteristics in amplitude and duration. Significant differences from baseline were found within the time interval between 15 and 22 s. In both cases, the HF component decreased immediately when an arousal occurs. However a larger decrement was observed during arousal associated with muscular activity. After that, HF returns slowly to the baseline. No significant differences

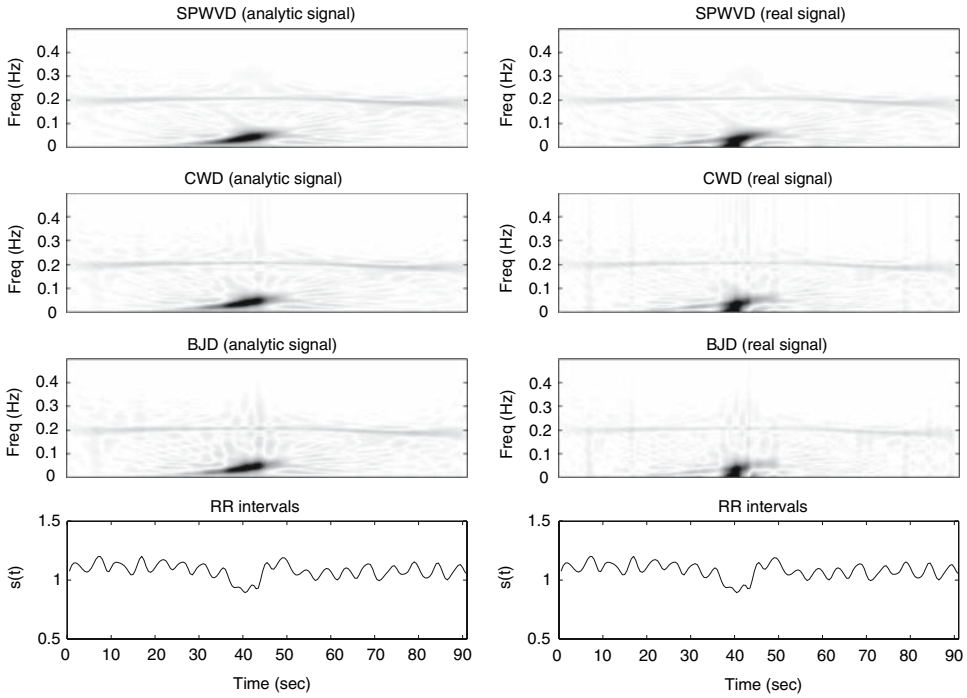

Fig. 3 Energy distribution of RR intervals during an arousal from sleep obtained with SPWVD, CWD and BJD. RR interval was analyzed as a real and analytic (after Hilbert transformation) sequences

with respect to baseline were found in any condition. LF component increased largely reaching its maximum close to the same time as RR value was minimum and going back to the baseline 25 s later, values were higher when muscular activity was present. Significant differences in respect to baseline were found in the time intervals between 15–26 and 19–22 s during both types of arousals. VLF component and LF/HF ratio showed a similar trend.

Comparison of the spectral indexes between arousals with and without muscular activity in specific time periods is shown in Figure 5. Patterns in both groups were the same. RR interval decreases in phase 1 with respect to the baseline. Then it increases during phase 2 and finally goes back to the baseline. Significant differences between the two classes of arousals were found only in phase 1. HF power decreases in phase 1 and presents a rise during phase 2 and returns to baseline during phase 3. Not significant differences were found between the two arousal groups. LF, VLF and LF/HF ratios show an increase during phase 1, whose values remain similar in phase 2. Finally in phase 3, they go back to the baseline. Statistical differences between the two groups of arousals occurred during phase 1.

4 Discussion

In the first part of this study, we compared different time-frequency distributions, smoothed pseudo Wigner–Ville, Choi–Williams and Born–Jordan distributions in order to identify the best one suited for the analysis of the HRV signal during arousals. Furthermore, the time-frequency analysis of the heart rate variability during spontaneous arousals in healthy obese subjects was carried on by applying SPWVD. Arousals were divided in to two groups: (1) arousals accompanied by muscular activity and (2) arousals without muscular activity.

From a methodological point of view, SPWVD, CWD and BJD show characteristics suitable for analyzing the time evolution of the HRV spectral features during arousal events. Even though the clearest energy representation is obtained when SPWVD is used, the other two distributions also allow distinguishing in a clear and comprehensible way at each time, the spectral content of the arousal events. For analytic signals, CWD and BJD do not retain the marginal properties and both show similar time-frequency representations and smoothed instantaneous power as SPWVD.

From the physiological point of view, arousals accompanied and not accompanied by muscular activity, present similar time evolution in the RR interval and spectral indexes. However, when a muscular activity takes place, a higher sympathetic activation is observed.

SPWVD displays cleaner time-frequency energy representation than BJD and CWD. Its smooth windows are able to eliminate almost completely the cross-terms, but SPVWD does not follow time by time the real value of the instantaneous power of the signal (as shown in Fig. 1).

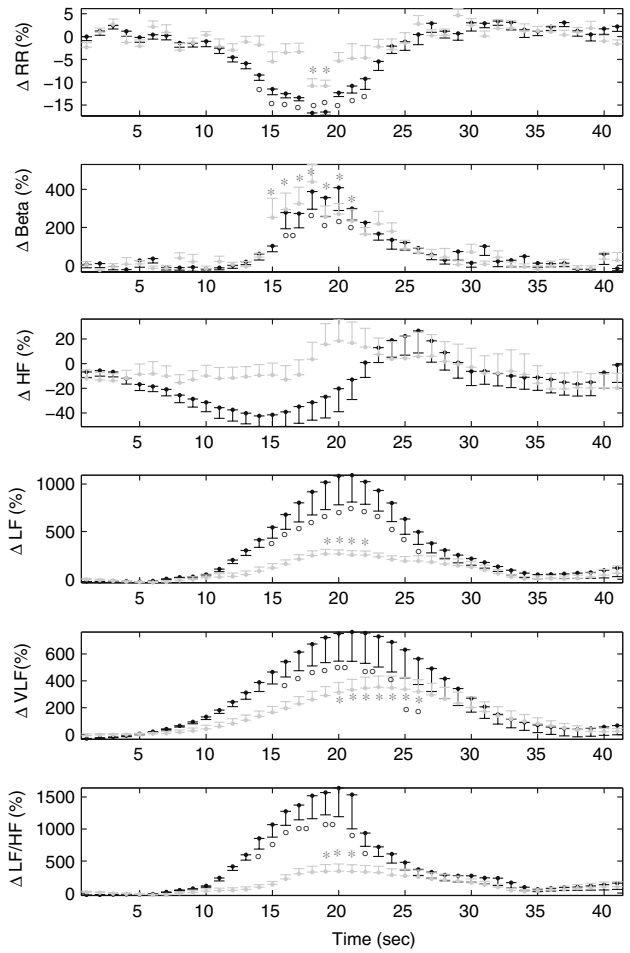

Fig. 4 Subject average of the heart-rate variability indexes during arousals from sleep. The average is obtained from 17 arousals with muscular activity (*black symbols* ° indicate significant difference with $p < 0.05$ vs baseline) and 14 without muscular activity (*gray symbols* * indicate significant difference with $p < 0.05$ vs baseline). From the top to the bottom, *RR* interval, cerebral β activity, *HF* high-frequency component, *LF* low-frequency component, *VLF* very low-frequency component and *LF/HF* low to high frequency ratio. Values are mean ± SE

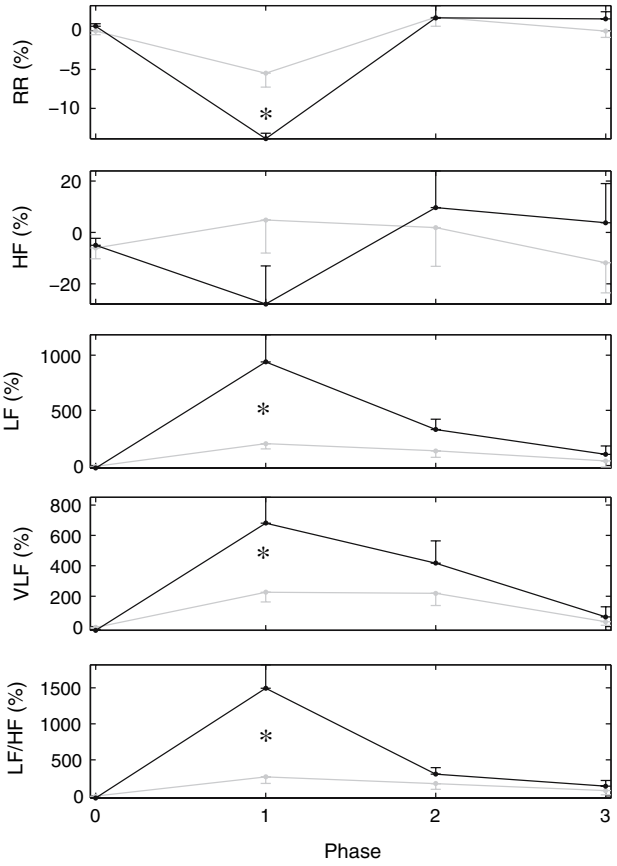

Fig. 5 Subject average of the heart rate variability indexes during arousals from sleep. The average is obtained from 17 arousals with muscular activity (*black symbols* ° indicate significant difference with $p < 0.05$ vs baseline) and 14 without muscular activity (*gray symbols* * indicate significant difference with $p < 0.05$ vs baseline). From the top to the bottom, *RR* interval, *HF* high-frequency component, *LF* low-frequency component, *VLF* very low-frequency component and *L/H* low to high frequency ratio. Values are mean ± SE. "0" average of five beats occurring 10 s before the RR minimum, "1" average of three beats centered around the RR minimum, "2" average of four beats occurring 5 s after the RR minimum and "3" average of ten beats occurring 15 s after RR minimum

Nevertheless, SPWVD tracks the changes in the frequency components with high time resolution, as it can be noticed in Fig. 1. Even if CWD and BJD did not display a clear time-frequency energy distribution, the auto-terms were completely identifiable with a good time and frequency resolution. BJD presents the greatest quantity of cross-terms, but as reported in literature and observed in Fig. 1, it is able to track well the exact instantaneous power of the signal. When an analytic signal is examined, the three TFDs show almost the same performances in the estimation of the instantaneous power. Therefore, it seems indifferent to use any of these distributions in such condition. This observation suggests that the major quantity of cross-terms is generated between the negative and positive frequencies at each time. Our study shows in a simple and practical way that the advantage of the analytic signal in order to minimize cross-terms when a multi-component signal is analyzed. A rigorous and interesting mathematical description is found in the papers presented by Schreier and Boashash [7, 38].

As final point, when spectral components of the HRV are studied in the time-frequency plane, it is not necessary to know the exact value of the power at each point, while it is important to detect the changes in the frequency components of the signal. Therefore, SPWVD could be a good option for the dynamical evaluation of the ANS action on HRV. However, also BJD and CWD are suitable for the analysis of HRV during transient events. Some papers describe comparative studies between the SPWVD, CWD and other distributions, remarking that the best analysis

approach depends on the self-features of the signal under study [12, 23, 26, 35].

Arousals may be linked to different sleep disturbances, such as periodic leg movements, restless-leg syndrome and sleep apnea. Physiological arousal can be related with alerting reactions that activate different body systems, such as the cardio-respiratory one, to cope with external stimuli. The nature of the spontaneous arousals could be seen as a vigilance system monitoring the external environment. However, due to the very close relation with sleep pathologies, arousal from sleep is seen as an indicator of sleep fragmentation and its quantification gives a clinical index of sleep quality [21].

Arousal responds differently to the specific causes of activation, and some other cerebral waves such as k-complexes and spindles seem to participate as primary form of arousal. For instance, some studies have found an increment is δ power during the breathing restore in OSA patients [2]. Then a hierarchical arousal response could be found and it depends on the efferent information towards the central nervous system. D-activations, k-complex and arousal produce different reactions of the autonomic nervous system depending on the requirements for overcoming a noxious event. k-complex produces a mild autonomic activation, while arousals generates very strong autonomic reaction [39]. In this way, an arousal with muscular activation suggests either greater vigilance state or powerful response than ones without muscular activation.

Characteristic changes in the heart rate have been reported previously in different physiological and pathological conditions. In conditions, where repetitive arousals occur, as cyclic alternating pattern [20] or periodic leg movement [41], a VLF component in the spectral components of the HRV signal appears, reflecting the influence of arousal repetition on HRV signal. A single arousal produces a large increment in the LF component, which suggests a major activation in the sympathetic activity, in order to reactivate some mechanisms of defense or alertness. Time-frequency approaches allow evaluating the time evolution of the sympatho-vagal balance with high time and frequency resolution. Time and frequency resolutions are defined in the kernel parameters. In SPWVD, the length of the independent (in time and in frequency) smoothing windows (kernel) defines the resolution. Length selection of these windows depends directly upon the characteristics of the signal in analysis. Proper selection of window lengths allows obtaining good time-frequency representations and the extraction of important information of interest. If a large frequency-smoothing window is selected, cross-terms are reduced but there is the risk of not discriminating the different frequencies. On the contrary, short frequency-smoothing window increases the resolution, but reduces the ability of eliminating cross-terms and consequently not clear time-frequency representations may be obtained.

Only few studies in literature have so far addressed the issue of using time-frequency approaches to analyze the HRV during arousal episodes. Our results are in agreement with the previous studies [8, 9, 33]. On the other hand, there are little discrepancies with the study by Blasi et al. [6], where the time evolution of the spectral parameters is analyzed. LF time activation and the time frame, in which, spectral indexes remain altered after arousal event, are much longer in [6] than in the present study. These disagreements could be produced by subject characteristics and/or arousal type. Infact, they considered evoked arousals while here only spontaneous ones are analyzed; this suggests that acoustic click could be responsible of an LF longer response since this process involves the activation and participation of the sensory system. Induced arousals seem to elicit different behavior in the ANS response; in fact, Sforza et al. [21] documented different autonomic responses in correspondence of different EEG events.

On the other hand, Smurra et al. [42] compared the feasibility of the visual scoring of the arousals using ASDA and UCL definitions (from the EEG and electromyography activity during NREM sleep). They found that arousals scored in the two methods were comparable in terms of concurrence and reproducibility. Vice versa, a clear difference between the two definitions is found when arousal is considered in terms of effects on HRV. The results of the present study suggest that arousals accompanied with chin activity (UCL definition) present a higher autonomic response during the phase of maximum tachycardia (see Fig. 5). Finally, the RR interval obtained with the presented protocol showed the typical pattern of tachy-bradycardia, when an arousal episode happens, alone or together with chin activity. In addition, significant differences found between the two groups of arousals suggest that major activation in the autonomic sympathetic activity takes place when external muscular activity also occurs.

In the last years, alternatives approaches to evaluate sleep have been developed, however, without taking arousals into account [10, 13]. Caffarel et al. [10] presented an interesting analysis between standard and automatic sleep staging, in which, they concluded that automatic sleep classification do not present robust measures as the gold standard. However, a previous detection of arousals could offer additional information to improve the automatic sleep staging. In addition, arousals could be evaluated by alternatives measures as that presented by Chen et al. [13]. In this study respiration and pulse rate are detected by a pillow sensor during sleep. Arousals could be assessed by this approach since when an arousal occurs, respiration and pulse rate present variations.

This study is limited to a small and specific sample of healthy subjects (obese), and a larger study in normal subjects is necessary. Furthermore, the selection of arousals was set-aside at sub-definition from the ASDA report. An extension of this protocol is necessary in order to include other definitions of arousals [21, 39]. Future work would include the analysis of arousals using time-frequency approaches in bi-variate form, in order to obtain maximum information from the interrelation among different signals, such as respiration and heart rate, during arousal events.

5 Conclusion

SPWVD, BJD and CWD demonstrated to be fine tools to evaluate the spectral parameters of the HRV during transient episodes such as arousals. For real signals, SPWVD seems to offer a simpler computation and clearer energy representation than BJD and CWD. When analytic signals are evaluated, it seems indifferent to use any distribution since their energy representations are extremely similar. Besides BJD lost its excellent properties when an analytic signal is used, this distribution presents a major time-frequency resolution than the other ones.

The results obtained in this study suggest that arousals accompanied by muscular activity are associated with greater sympathetic activation than arousals without muscular activity in sleep stage 2, although the duration of the tachy-bradycardia and recovery time were similar.

Acknowledgments This paper was partially supported by the My-Heart Project IST 507816 of the European Community and by CONACyT (Mexico), grant 169435/205104.

References

1. Atlas task force of American sleep disorders association (1992) EEG arousal: scoring rules and examples. Sleep 15:174–184
2. Berry RB, Asyaly MA, Mcnellis MI, Khoo MC (1998) Within night variation in respiratory effort preceding apnea termination and EEG delta power in sleep apnea. J Appl Physiol 85:1434–1441
3. Bianchi AM, Bontempi B, Cerutti S, Gianoglio P, Comi G, Natali MG (1990) Spectral analysis of heart rate variability signal and respiration in diabetic subjects. Med Biol Eng Comput 28:205–211
4. Bianchi AM, Mainardi LT, Petrucci E, Signorini MG, Cerutti S (1993) Time-variant power spectrum analysis for the detection of transient episodes in HVR signal. IEEE Trans Biomed Eng 40:136–144
5. Bianchi AM, Mainardi LT, Cerutti S (2000) Time-frequency analysis of biomedical signals. Trans Inst Meas Control 22:215–230
6. Blasi A, Jo J, Valladares E, Morgan BJ, Skatrud JB, Khoo CKM (2003) Cardiovascular variability after arousal from sleep: time-varying spectral analysis. J Appl Physiol 95:1394–1404
7. Boashash B (1995) Note the Use of the Wigner distribution for time-frequency signal analysis. IEEE Trans Signal Process 43:1262–1268
8. Bonnet MH (1989) The effect of sleep fragmentation on sleep and performance in younger and older subjects. Neurobiol Aging 10:21–25
9. Bonnet MH, Arand DL (1997) Heart rate variability: sleep stage, time of night, and arousal influences. Electroencephalogr Clin Neurophysiol 102:390–396
10. Caffarel J, Gibson GJ, Harrison JP, Griffiths CJ, Drinnan MJ (2006) Comparison of manual sleep staging with automated neural network-based analysis in clinical practice. Med Biol Eng Comput 44:105–110
11. Catcheside PG, Chiong SC, Orr RS, Mercer J, Saunders NA, McEvoy RD (2001) Acute cardiovascular responses to arousal from non-REM sleep during normoxia and hypoxia. Sleep 24:895–902
12. Chan HL, Huang HH, Lin JL (2001) Time-frequency analysis of heart rate variability during transient segments. Ann Biomed Eng 29:983–996
13. Chen W, Zhu X, Nemoto T, Kanemitsu Y, Kitamura K, Yamakoshi K (2005) Unconstrained detection of respiration rhythm and pulse rate with one under-pillow sensor during sleep. Med Biol Eng Comput 43:306–312
14. Choi HI, Williams WJ (1989) Improved time-frequency representation of multicomponent signals using exponential kernels. IEEE Trans Acoust Speech Signal Process 37:862–871
15. Cohen L (1966) Generalized phase-space distribution functions. J Math Phys 7:781–786
16. Cohen L (1989) Time-frequency distributions: a review. Proc IEEE (77):941–981
17. Collard P, Dury M, Delguste P, Aubert G, Rodenstein D (1996) Movement arousals and sleep-related disordered breathing in adults. Am J Respir Crit Care Med 154:454–459
18. Davies RJ, Belt PJ, Roberts SJ, Ali NJ, Stradling JR (1993) Arterial blood pressure responses to graded transient arousal from sleep in normal humans. J Appl Physiol 74:1123–1130
19. Driscoll DM, Meadows GE, Corfield DR, Simonds AK, Morrell MJ (2004) Cardiovascular response to arousal from sleep under controlled conditions of central and peripheral chemoreceptor stimulation in humans. J Appl Physiol 96:865–870
20. Ferini-Strambi L, Bianchi A, Zucconi M, Oldani A, Castronovo V, Smirne S (2000) The impact of cyclic alternatine pattern on heart rate variability during sleep in healthy adults. Clin Neurophysiol 111:99–101
21. Halasz P, Terzano M, Liborio P, Bodizs R (2004) The nature of arousal in sleep. J Sleep Res 13:1–13
22. Hlawatch F, Boudreaux-Bartel G (1992) Linear and quadratic time-frequency signal representations. IEEE Signal Process Mag 21–67
23. Hlawatsch F, Manickam TG, Urbanke RL, Jones W (1995) Smooth pseudo-Wigner distribution, Choi–Williams distribution, and Cone-kernel representation: ambiguity-domain analysis and experimental comparison. Signal Process 19:149–168
24. Jasson S, Medigue C, Maison-Blanche P, Montano N, Meyer L, Vermeiren C, Mansier P, Coumel P, Malliani A, Swynghedauw B (1997) Instant power spectrum analysis of heart rate variability during orthostatic tilt using a time-/frequency-domain method. Circulation 96(10):3521–3526
25. Jeong J, Williams WL (1992) Kernel design for reduced interference distributions. IEEE Trans Signal Process 40:2402–2412
26. Karlsson S, Yu J, Akay M (2000) Time-frequency analysis of myoelectric signals during dynamics contractions: a comparative study. IEEE Trans Biomed Eng 47:228–238
27. Khadra LM, Dridi JA, Khasawneh MA, Ibrahim MM (1998) Time-frequency distributions based on generalized cone-shape

kernels for the representation of nonstationary signals. J Franklin Inst 33B:915–928
28. Mainardi LT, Bianchi AM, Cerutti S (2002) Time-frequency and time-varying analysis for assessing the dynamic response of cardiovascular control. Crit Rev Biomed Eng 30:175–217
29. Malliani A (1999) The pattern of sympathovagal balance explored in the frequency domain. News Physiol Sci 14:111–117
30. Martin W, Flandrin P (1985) Wigner–Ville spectral analysis of nonstationary process. IEEE Trans Acoust Speech Signal Process 33:1462–1470
31. Martin SE, Engleman HM, Deary IJ, Douglas NJ (1996) The effect of sleep fragmentation on daytime function. Am J Respir Crit Care Med 153:1328–1332
32. Montano N, Ruscone TG, Porta A, Lombardi F, Pagani M, Malliani A (1994) Power spectrum analysis of heart rate variability to assess the changes in sympathovagal balance during graded orthostatic tilt. Circulation 90(4):1826–1831
33. Morgan B, Crabtree D, Puleo D, Skatrud J (1996) Neurocirculatory consequences of abrupt change in sleep state in humans. J Appl Physiol 80:1627–1636
34. Novak P, Novak V (1993) Time/frequency mapping of heart rate, blood pressure and respiratory signals. Med Biol Eng Comput 31:103–110
35. Pola S, Macerata A, Edmin M, Marchesi A (1996) Estimation of the power spectral density in nonstationary cardiovascular time series: assessing the role of the time-frequency representations (TFR). IEEE Trans Biomed Eng 43:46–59
36. Ramos G, Carrasco S, Medina V (2000) Time-frequency analysis of the heart rate variability during Valsalva manoeuvre. J Med Eng Technol 24:73–82
37. Rechtschaffen A, Kales AE (1968) A manual of standardized terminology, techniques and scoring system for sleep stages of human subjects. Brain Information Services/Brain Research Institute, UCLA
38. Schreier PJ, Scharf LL (2003) Stocastic time-frequency analysis using the analytic signal: why the complementary distribution matters. IEEE Trans Signal Process 51:3071–3079
39. Sforza E, Jouny C, Ibanez V (2000) Cardiac activation during arousal in humans: further evidence for hierarchy in the arousal response. Clin Neurophysiol 111:1611–1619
40. Sforza E, Chapotot F, Lavoie S, Roche F, Pigeau R, Buguet A (2004) Heart rate activation during spontaneous arousals from sleep: effect of sleep deprivation. Clin Neurophysiol 115(11):2242–2251
41. Sforza E, Pichot V, Barthelemy JC, Haba-Rubio J, Roche F (2005) Cardiovascular variability during periodic leg movements: a spectral analysis approach. Clin Neurophysiol 116:1096–1104
42. Smurra MV, Dury M, Aubert G, Rodenstein DO, Liistro G (2001) Sleep fragmentation: comparison of two definitions of short arousals during sleep in OSAS patients. Eur Respir J 17:723–727
43. Spicuzza L, Bernardi L, Calciati A, Ugo di Maria G (2003) Autonomic of heart rate variability during obstructive versus central apneas in patients with sleep-disorders breathing. Am J Resp Crit Care Med 167:902–910
44. Stankovic L (1996) Auto-term representation by the reduced interference distributions: a procedure for kernel design. IEEE Trans Signal Process 44:1557–1563
45. Task force of the European Society of Cardiology and the North American Society of Pacing and Electrophysiology (1996) Heart rate variability: standards of measurement, physiological interpretation, and clinical use. Circulation 93:1043–1065
46. Trinder J, Merson R, Rosenberg JI, Fitzgerald F, Kleiman J, Bradley TD (2000) Pathophysiological interactions of ventilation, arousals, and blood pressure oscillations during Cheyne–Stokes respiration in patients with heart failure. Am J Respir Crit Care Med 162:808–813
47. White DP (2006) Sleep apnea. Proc Am Thorac Soc 3:124–128
48. Young T, Peppard PE, Gottlier DG (2002) Epidemiology of obstructive sleep apnea, a population health perspective. Am J Respir Crit Care Med 165:1217–1239